Galaxy potentials and orbit integration

Andrés García-Serra Romero

Universidad de la Laguna, Astronomy and Astrophysics master's degree.
e-mail: alu0101451923@ull.edu.es

ABSTRACT

Aims. In this work we will be trying to explain the behavior of different mass stellar populations in the Milky Way, integrating their orbits and using parameters of this orbits to explain the different patterns these could show.
Methods. Gaia *EDR2* data will be used to perform this calculations, with which we will use `gala` python package to perform orbit integration and extract the necessary parameters.
Results. Older populations of stars tend to have more chaotic, slower, and higher eccentricity trajectories. This may be caused by their interaction during time with dust, gas and other elements of the galaxy. Younger star populations tend to have close to circular eccentricities, with less circular velocity dispersion and are mostly located in the thinner part of the galaxy disk.

Key words. Orbit integration - GAIA - Stellar populations - Eccentricity - Star dynamics - Galaxy potential

1. Introduction

Gravitational interactions are the main source for stars and, in general, bounded systems to move. This govern the way objects orbit around each other. Not only complex and bigger systems like galaxies or galaxy groups, also in smaller scale like local systems or our own solar system.

In this way, studying this gravitational forces can teach us a lot in the matter of how every star is moving in a galaxy. Keep in mind that for us to theoretically solve or compute a system as complex as a galaxy will take a lot of time in the making and will not be worthy, because modeling this systems in a more general ambit is much more optimum knowing that these models can reach high levels of accuracy.

The gravitational potential we are referring to when talking about gravitational interaction is determined by the quantity of mass held inside it, as well as the distribution of this mass, the density profile of baryonic matter of a galaxy obviously plays an important role in its potential. The classical definition of this potential id the following:

$$\Phi(x) = -G \int_0^V \frac{\rho(x')}{x' - x} d^3x'$$

Being V the complete volume in which this potential can be calculated. As we know, the gravitational field is defined as the gradient of this potential, and the force will be then the gravitational field times the mass which is being pulled, following:

$$F(x) = -m \cdot \nabla\Phi(x)$$

Using this definitions we can obtain the expressions of the Poisson potential (useful when wanting to obtain the density profile of any potential) and the circular velocity:

$$\nabla^2\Phi(x) = 4\pi G\rho(x) \quad , \quad v_c(r) = \sqrt{\frac{\partial\Phi}{\partial r} r}$$

Thus, knowing the mass distribution of a galaxy and its density profile lets us model the circular velocity of stars in it at different radii. Also, the other way around, stellar movement around galaxies can confirm our potential models of galaxies are correct.

This is what we will do in this project, using stellar velocities data and different models we will see the behavior of these and how they perform. To do this we basically split the galaxy morphology in different parts that will bring different potentials to the equation. Using all these potentials together will help us model these galaxies in a better way than finding a very complex potential that behaves as one.

1.1. The Milky Way

The Milky way can be divided in 4 of these potentials to treat separately. To model the bulge, nucleus and baryonic halo we normally use spherical potentials, where as to model the disk flattened potentials are used. We will be now presenting these potentials in a list.

For the disk of the galaxy the Miyamoto-Nagai potential is used. This follows axial symmetry and depends on two main scale parameters, a for the radius and b for the vertical coordinate.

$$\Phi(r) = -\frac{GM}{\sqrt{r^2 + (a + \sqrt{z^2 + b^2})^2}}$$

For the nucleus and the central bulge of the galaxy the Hernquist potential is being used, which follows spherical symmetry. This one depends also on a scale parameter a and a constant ρ_0.

$$\Phi(r) = -4\pi G\rho_0 a^2 \frac{1}{1 + r/a}$$

Finally the Navarro, Frenk & White (NFW) potential is being used for the baryonic halo. This potential follows spherical symmetry and was obtained via simulations.

$$\Phi(r) = -4\pi G\rho_0 a^3 \frac{ln(1 + r/a)}{r}$$

With these potentials we can construct the whole Milky Way potential summing them. Once we have this, we can apply it to any star with just its phase space initial conditions to know its orbit. This will allow us to trace the trajectory of stars, obviously knowing that any other gravitational interactions haven't been taken into account.

2. Methodology

Now that we have the basics covered we can jump straight to the data and orbit integration process. For this part, we will be following a Python notebook [1] made for computing galactic orbits for Milky Way stars. In this section we will explain briefly the different code sections used.

2.1. Data query and coordinate transformation

Firstly, we will need to obtain the data, for this we will use the tool `astroquery`, which allows us to download data from different queries in a very intuitive way. Our requirements for the query were simple, in first place, we will be using *Gaia EDR2* data, which is data from the gaia satellite in its second data release. Then, 4096 galaxies will be selected, with distance from the sun at maximum 100 pc (`parallax > 10`) and a signal-to-noise ratio greater than 10 (`parallax_over_error > 10`). Finally we will ask for stars with radial velocity data, via `"radial_velocity IS NOT null"`.

From these stars we will ask for their magnitudes in different bands (G, BP, RP), coordinates, radial velocities and proper motion components.

Now we need to transform the coordinates of the data from heliocentric spherical values to galactocentric cartesian values. This will be performed using the `astropy.coordinates` tool, which is very useful in this cases. For doing this we will assume a distance from the Sun to the center of the galaxy of $d_\odot$=8.1 kpc, as found by the GRAVITY collaborations [2], and a vertical coordinate of the sun $z_\odot \approx 0$.

2.2. High and low mass stellar populations

What we want to do at the end is computing stellar orbits of different populations of stars to use this circular velocity data as an indicator of the type of the star we are working with. Then we could correlate their position inside the galaxy with its age and metallicity. To do this we will firstly make a selection of two different groups using the mass as criteria. As we know, more massive stars tend to have a shorter life while less massive ones live longer.

To make this separation we will use a color magnitude diagram (CMD) with the magnitude data we have. We will be using M_G as the vertical axis and the colour index $M_{BP} - M_{RP}$ as the horizontal axis. Inside the CMD, most massive stars will have a higher value of absolute magnitude and a lower value of the colour index, while less massive ones will have the opposite behavior.

Knowing this we set the limits at: $0.5 < BP - RP < 0.7$ and $2 < M_G < 3.75$ for the high mass young stars, and $2 < BP - RP < 2.4$ and $8.2 < M_G < 9.7$ for the low mass old stars.

This selection criteria is shown in figure 1, where we plotted the resultant ~600 old less massive stars and the ~200 young more massive stars.

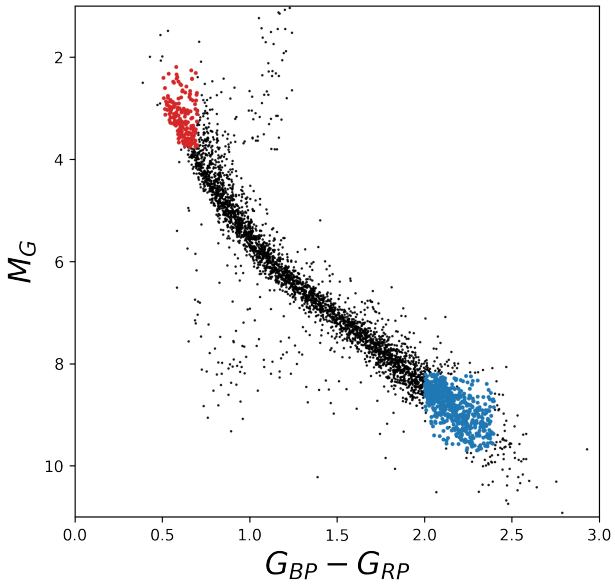

Fig. 1. Color magnitude diagram of the data downloaded. In red, most massive young stars. In blue, less massive old stars.

3. Numerical iteration of stellar orbits

For the orbit integration we will be using the `gala` package, which allows us to study the galactic dynamics of stars. For doing this we will need to set some initial parameters to the potential models used by default.

This parameters will vary with the different potentials we used for each part of the galaxy, as we mentioned in the introduction (see 1.1). This parameters can be found in table 1.

Table 1. Default parameters of scale for the different region potentials in the galaxy model.

Region	Nucleus	Bulge	Disk	Halo
Potential	Hernquist		Miyamoto-Nagai	NFW
M ($M_\odot$)	$1.71 \cdot 10^9$	$5 \cdot 10^9$	$6.8 \cdot 10^{10}$	$5.4 \cdot 10^{11}$
a	0.07	1.0	3.0	15.62
b	0.28	/	0.28	/

To plot this stars trajectories we only have to calculate de Hamiltonian of the potential and use gaia data to set initial

phase space conditions.Then we can select one star of each sample and reproduce the projections of its orbit. We did this in the XY plane, the YZ plane and the YZ plane. The projections of the orbit are shown in galactocentric coordinates and can be checked in figure 2. In this case we used a time integration of 500 Myr.

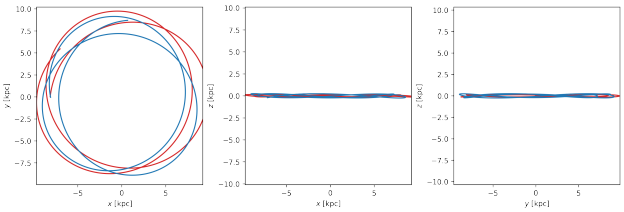

Fig. 2. Trajectory of different mass stars in XY, XZ, YZ planes computed for 500 Myr. In red the high mass star, in blue the low mass star. Bigger version of the image in Appendix.

Then we plotted the same for a time integration of 2000 Myr, which can be seen in figure 3.

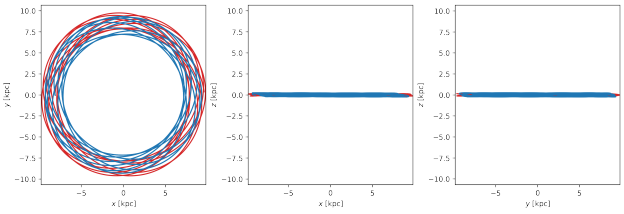

Fig. 3. Trajectory of different mass stars in XY, XZ, YZ planes computed for 2000 Myr. In red the high mass star, in blue the low mass star. Bigger version of the image in Appendix.

All these plots will be at the end of the document in a bigger size for a better inspection (see Appendix).

4. Study of dynamics characteristics in different stellar populations

Now we can analyze closely both stellar populations of higher and lower mass in different dynamics parameters, like $z_{\max}$, ϵ or the apocenter and pericenter.

4.1. Maximum height over the galactic plane (z_{max})

The first parameter we will be focusing on is the maximum height that each star will reach in its trajectory over the galactic plane, $z_{\max}$. The histogram of the $z_{\max}$ value over both populations is performed and shown in figure 4.

As we can see in the histogram, lower mass stars tend to have higher $z_{\max}$ values in comparison to higher mass stars. This could confirm that higher mass young stars are born in the galactic disk and fall into the thick disk or the baryonic halo via interactions, it could also mean that older low mass stars could be born farther than the galactic disk.

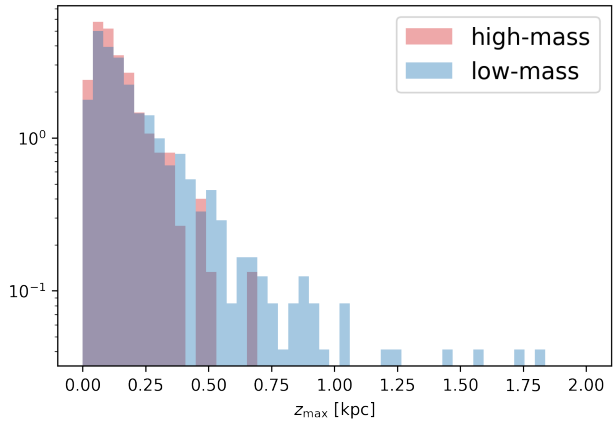

Fig. 4. Histogram of maximum height over z plane. In red, most massive young stars. In blue, less massive old stars.

4.2. Eccentricity (ϵ)

We can now study the distribution of the histograms for the different eccentricities for our data. This histogram is shown in figure 5.

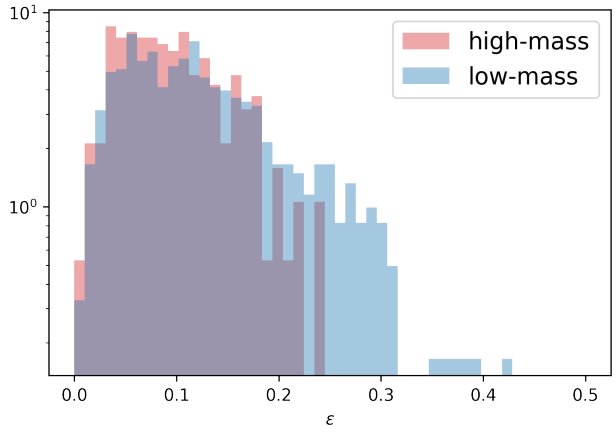

Fig. 5. Histogram of eccentricities of the orbits. In red, most massive young stars. In blue, less massive old stars.

We can clearly see how lower mass old stars reach higher eccentricities than higher mass young stars. This can be explained. This behavior can confirm the previous data, in which we saw that they also reached higher z values. This could mean that these old young stars can reach farther orbits. TO check this we can perform a last histogram for the apocenter and pericenter of these stars.

4.3. Apocenter and pericenter

Finally, to check the different trajectories present in both populations we can make an histogram on the closest point of orbit (pericenter) and the farthest point of orbit (pericenter) of every star on both populations. This histograms are shown in figures 6 and 7.

These final plots confirm what we were expecting. For both of them we can see how lower mass old stars tend to have wider orbits, not only get farther from the center of the galaxy, they also get closer. This is coherent to the fact that these lower mass stars also have higher $z_{\max}$ values, which make their orbits more

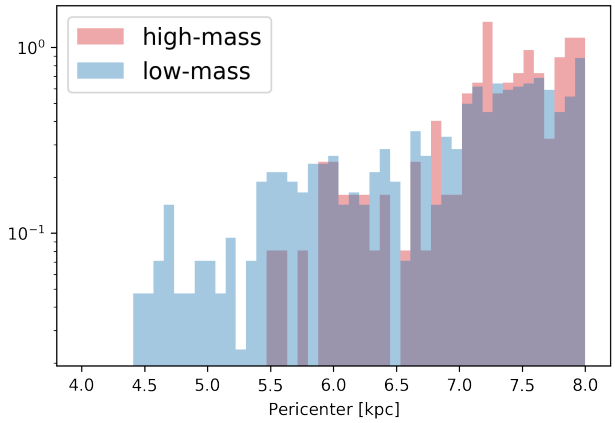

Fig. 6. Histogram of pericenters of the orbits. In red, most massive young stars. In blue, less massive old stars.

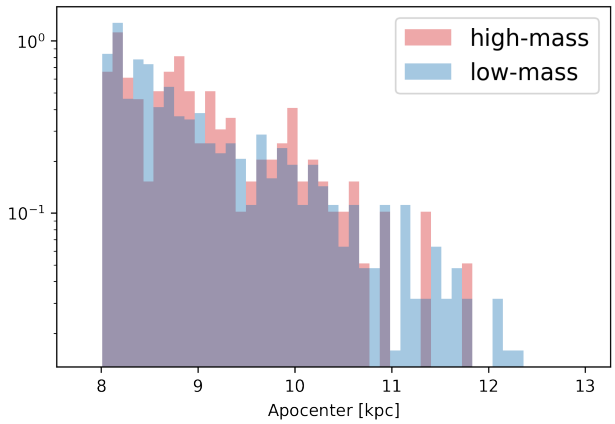

Fig. 7. Histogram of apocenters of the orbits. In red, most massive young stars. In blue, less massive old stars.

scattered in every coordinate.

To confirm this information we plotted the result of the integration of every orbit for both popullations, which is shown in figure 8. A bigger size version of the figure is shown at the end of the document (see Appendix).

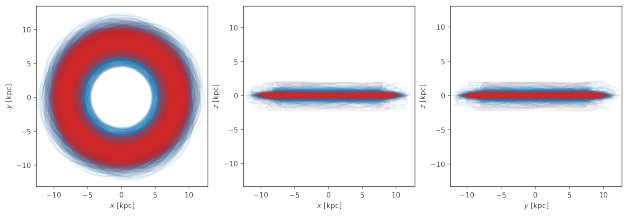

Fig. 8. Trajectory of different mass stars in XY, XZ, YZ planes computed for 2000 Myr for every star per sample. In red the high mass stars, in blue the low mass stars. Bigger version of the image in .

This finally confirms the point made, low mass old stars tend to have more scattered trajectories in every direction, as we can see in this figure, for the XY plane the trajectories which correspond to these stars (blue) are wider to the ones of earlier stars (red). Also in the rest of the planes represented higher mass stars tend to be condensed next to the galactic plane.

5. Discussion and conclusions

During all the project we have seen that lower mass stars have a wider range of trajectories in the space, meaning they can reach closer and farther distances from the central region of the galaxy, as well as in the z axis. This low mass stars are closely related to older stars, meaning then that stars tend to be created in the disk closely to the galactic plane, and with different interactions during its life period some of them can shift to farther regions of the disk, having a bigger trajectory and increasing their eccentricity.

It is true that lower mass stars doesn't have to be older, but in their sample there will be much more old stars than in the higher mass sample. This is because the life of higher mass stars is much shorter. This is way in every point made during the work we referred to the less massive stars as old ones and more massive stars as young ones.

Having this in mind, we could think that the argument of stars being shifted to farther regions during its life doesn't make any sense because older stars could have time to be shifted and then attracted to the most energy stable region of the galaxy which is in the disk next to the galactic plane. We never see this happen because the time scale for a star to overcome this shift and rejoin the thinner disk region is higher than the galaxy life time itself, so they will never be capable of returning to their original trajectories.

This shift effect by interactions with other stars, dust and gas can also be explained by the fact that every one of this interactions slows down the orbit of a star, making it have a larger radius of orbit and a higher eccentricity.

5.1. Conclusions

During this work we were capable of using free source data paired with python software tools to analyze different mass stars populations in order to study the behavior of their orbits.

The behavior of both populations was as expected and discussed in the previous section, older stars tend to have slower and higher eccentricity orbits around the galaxy, whereas younger stars tend to be created and stay in the thinner part of the galaxy disk, being this the most stable region.

To arrive at this conclusion we have studied different parameters like the apocenter and pericenter of each integrated trajectory and their maximum z coordinate. In each and every one of this parameters we arrived to the same conclusion, also known in the bibliography.

6. References

[1] Adrian Price-Whelan, Stephanie T. Douglas. *Computing Galactic Orbits of Stars with Gala.* URL: https://learn.astropy.org/tutorials/gaia-galactic-orbits.html

[2] Abuter, R et al. *Detection of the gravitational redshift in the orbit of the star S2 near the Galactic centre massive black hole.* URL: http://dx.doi.org/10.1051/0004-6361/201833718

Appendix: Bigger size images

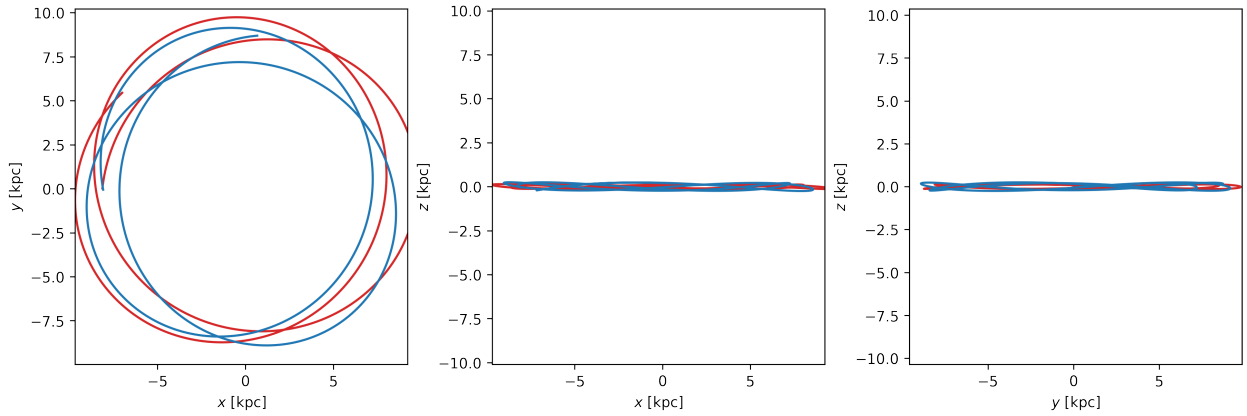

Fig. 9. Trajectory of different mass stars in XY, XZ, YZ planes computed for 500 Myr. In red the high mass star, in blue the low mass star.

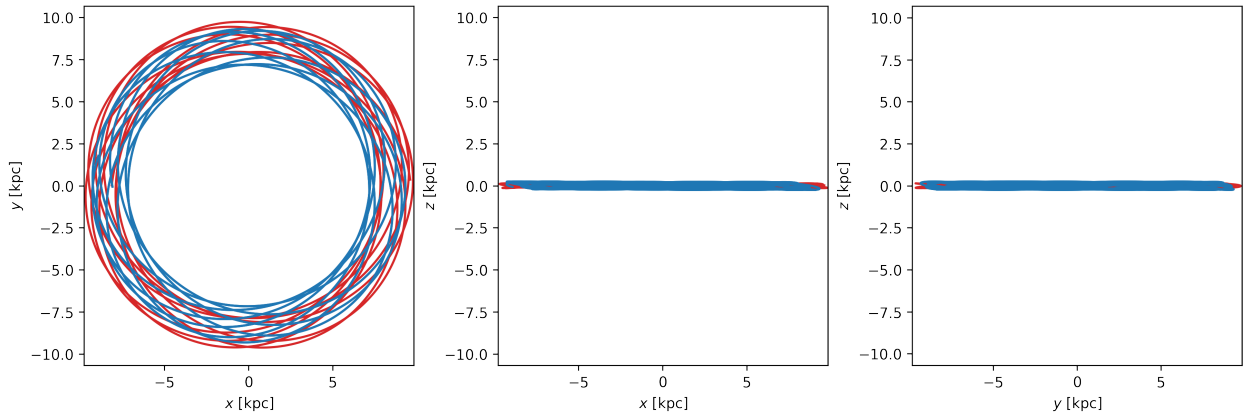

Fig. 10. Trajectory of different mass stars in XY, XZ, YZ planes computed for 2000 Myr. In red the high mass star, in blue the low mass star.

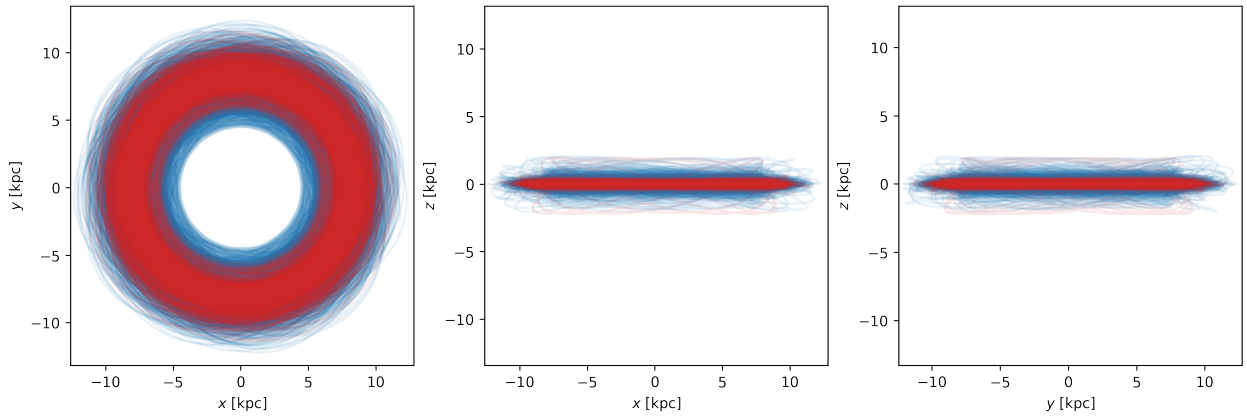

Fig. 11. Trajectory of different mass stars in XY, XZ, YZ planes computed for 2000 Myr for every star per sample. In red the high mass stars, in blue the low mass stars.